Length Scales and Dynamics in the Reorientational Relaxation of Tracers in Molecular and Polymeric Glass Formers via Electron Spin Resonance Spectroscopy

Laura Andreozzi, Massimo Faetti,* Marco Giordano, and Fabio Zulli

Dipartimento di Fisica 'Enrico Fermi', Università di Pisa, Largo Bruno Pontecorvo 3, I-56127 Pisa, Italy

Received: July 21, 2010; Revised Manuscript Received: September 2, 2010

It is widely accepted that a temperature region exists above the glass transition temperature, playing a fundamental role in the physics of polymers and glass formers. In this region, several dynamic crossovers have been experimentally and numerically revealed in the past years and the onset of glassy behavior is generally located, because of cooperative and heterogeneous features exhibited by the dynamics. In this Article, the rotational dynamics of two different stiff molecular spin probes dissolved in poly(propylene glycol) has been investigated by electron spin resonance spectroscopy in a wide temperature range. Decoupling phenomena between macroscopic and microscopic transport properties have been observed in the crossover region. A comparison with previous studies carried out with the same tracers dissolved in different polymers and glass formers strongly supports the idea that the observed crossover signals the onset of spatial correlations of dynamics on the length scale probed by the tracers.

1. Introduction

The most salient feature of glass former dynamics is undoubtedly the dramatic slowing of molecular motion as the glass transition is approached from above, notwithstanding the static structure of the glass is virtually coincident with that of the corresponding liquids.[1,2] This is highlighted by the behavior of the structural relaxation time (or that of shear viscosity) that enormously increases, usually in a super-Arrhenius way, during the vitrification process. The origin of this slowing of dynamics is a long-standing issue in condensed matter physics,[1,2] and, even if significant progresses have been made in our understanding of relaxation dynamics of glass formers in the past few years,[3−7] a clear and widely accepted explanation for such a peculiar behavior is still lacking. Instead, a variety of different theoretical approaches have been developed, which often appear at odds with one another. This is very unpleasant, because the "anomalous slowing" of dynamics in glass-forming systems is general enough to deserve description by a universal theory. Indeed, because of this universal character of the glass transition, the largest part of the proposed theoretical approaches foresees the existence of a underlying either thermodynamic[8−12] or dynamic[13−16] critical point, postulated to be either avoided[9,13] (for the models predicting singularity above the experimental glass transition temperature T_g) or unreachable[8,10−12,14,16] (when the singularity is expected below T_g).

Moreover, independently of the prediction ability of these models, it is widely accepted that there is a temperature region above the experimental T_g that plays a central role for a complete understanding of the glass transition phenomenon.[17,18] This region, named the crossover region, is characterized by distinctive changes in the dynamical properties of the glass formers such as changes in the Vogel−Fulcher parameters characterizing the temperature dependence of the α relaxation time, decoupling phenomena between microscopic and macroscopic transport properties, the $\alpha-\beta$ splitting, and changes in the frequency-dependent calorimetric data.[19−31] In this region, the critical temperature of the mode coupling theory[13] is usually found, and, according to several numerical studies, a different way of sampling the energy landscape sets in.[32−36]

A common physical reason for all of these anomalies is suggested by the finding that crossover temperatures obtained with such different experimental methods are often comparable for a given material. An old idea is that these changes are related to the onset of molecular cooperativity and dynamical heterogeneities.[24,37−40] Even if not fully equivalent,[41,42] these two concepts are strongly related and often used synonymously to indicate the increasingly correlated nature of dynamics in glass-forming systems on approaching T_g. It is understood that the specificity of the different systems should be also considered. In polymers, due to the existence of the long chains that allow for relaxation modes, it is probably more intuitive the picture of cooperative effects, whereas for low molecular liquids it appears quite simple the picture of dynamic heterogeneities as clusters of more or less mobile molecules with effects that are only intermolecular in character. These dynamical correlations have been observed with different experimental techniques and numerical simulations,[40−46] and all the data provided length scales of the order of few nanometers at the glass transition. Referring to polymeric glass formers, of main interest in this work, it should be emphasized that the existence of a broad spectrum of dynamics processes effective at different time and length scales also appears as a natural consequence of the macromolecular nature of the system.[47,48] From a theoretical point of view, due to the complex architecture of the macromolecular structure, the dynamic properties of polymeric chains are usually described focusing on universal features through coarse graining procedures.[49] The most popular model is the Rouse model[49] where, after coarse-graining, the chains are treated as a series of beads connected by elastic springs and subjected to Brownian forces. A set is found of intrachain relaxation modes characterized by different length scales and relaxation times. Despite the crude assumptions and approximations, the Rouse model is usually able to provide a quantitative description of many dynamic properties of polymer melts of molar mass lower than a critical value.[48−50] For higher molar mass polymers, topological con-

* To whom correspondence should be addressed. Telephone: +390502214508. Fax: +390502214890. E-mail: massimo.faetti@df.unipi.it.

10.1021/jp106798c
Published on Web 09/22/2010

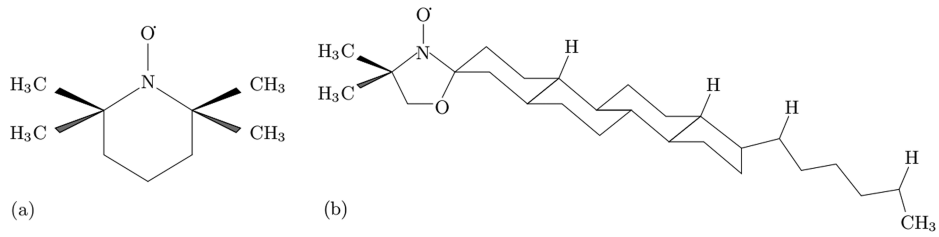

Figure 1. Structure of the TEMPO (a) and cholestane (b) spin probes.

straints related to the macromolecular nature must be taken into account, and, in the dynamics of the system, new effects appear that are modeled, for example, introducing the reptation concept.[49] With reference to the Rouse approach, shortcomings of the model and deviation from the predictions have been found in both numerical and experimental works.[51−54] The main flaws concern the length scale smaller than the nanometer where local stiffness and other specific local properties probably play a fundamental role, and the short-time regime of the global chain dynamics that evidences major discrepancies from the models predictions, especially in the crossover region.

From the previous considerations, it is understood the reason why molecular probe spectroscopies are a useful investigation method in general and in particular to study the crossover dynamic region of glass formers systems. Among them, electron spin resonance (ESR) has shown its ability in detecting dynamic crossovers in supercooled liquids and polymers.[23,25−28] In fact, sensitivity to the selected length scale can be obtained by dissolving paramagnetic tracers of proper size and shape in the investigated diamagnetic glass formers. On the other hand, it is well-known the great sensitivity of the ESR line shape to the details of the molecular reorientation in the so-called slow motional regime of the paramagnetic system, which usually characterizes reorientational dynamics in the crossover region of glass formers.[55−61]

In this work, ESR experiments on the rotational dynamics of two different paramagnetic probes dissolved in a poly(propylene glycol) matrix are reported. Different dynamical regimes were found with crossover temperatures. Similarities and differences in the behavior of different probes were discussed in terms of heterogeneous and cooperative dynamics. Moreover, the results are discussed with reference to previous data pertaining to the rotational diffusion of the same tracers dissolved in other glass formers.

2. Experimental Methods

In a typical continuous wave X-band ESR experiment, a static magnetic field B resolves the Zeeman degeneracy of the spin system, whereas a low intensity microwave field, linearly polarized in a plane perpendicular to B, induces σ transitions between the Zeeman levels. In the linear response regime, the ESR spectrum is related to the Laplace transform of the autocorrelation function of the transverse component of the magnetization M_x.[55,56] In dilute systems, the line shape depends on the rotational dynamics of paramagnetic probes because the main magnetic interactions, the Zeeman and Hyperfine ones, are anisotropic in character, with their principal axis fixed in a molecular frame, whereas the electron spin is quantized along the static field direction. Thus, tracer reorientation results in local magnetic fields fluctuating at the microscopic times, which relax the magnetization and broaden the resonance. The analysis of the ESR spectra is well established, and different numerical approaches are usually employed depending on the time scale that characterizes the spin probe dynamics.[55−62] The rotational dynamics is modeled in terms of proper stochastic processes expanding the conditional probability for the molecular orientation $P(\Omega,t|\Omega_0,t_0)$ in terms of the Wigner matrices. Different from other spectroscopies probing rotational dynamics, which are sensitive to the fluctuations of Wigner matrices of rank 1 (dielectric spectroscopy, infrared spectroscopy) or 2 (Raman, depolarization of fluorescence, Kerr effect), ESR spectroscopy, in the so-called slow motion regime, depends on the fluctuation of the Wigner matrices of every even rank, having so a greater sensitivity to the detail of the reorientational mechanism.[56−60] In this dynamical region, we employed the analysis method of the ESR spectra developed by using the generalized Mori projection tecnique.[56,57] When the time scale of rotational motion becomes slower, the ultraslow regime is found where the ESR line shape results to be largely independent of molecular dynamics. A careful analysis of the spectrum with proper algorithms[62] is necessary to obtain the magnetic parameters values, assumed independent of temperature, characterizing the paramagnetic tracers. It is important to point out that the limit where the ultraslow regime really sets in for the X-band ESR spectroscopy is not determined in a simple way, even if one considers a specific molecular probe. For example, the values of $10^{-7}-10^{-6}$ s, which in the literature are referred to the nitroxide spin probes, are only indicative and should be taken with care. We have shown[28,63] that, thanks to the high stability of the static magnetic field, a high-resolution experimental procedure can be employed, allowing one to follow the rotational dynamics also when the correlation times are of a few microseconds. Such a procedure was adopted in this study for the spin probe cholestane at low temperatures.

The ESR experiments were carried out with a Bruker ER200D spectrometer equipped with an X band bridge and a NMR gaussmeter ER035M. The temperature was controlled with a gas-flow variable temperature unit with stability of 0.1 K.

The two paramagnetic molecular tracers used for this study belong to the family of nitroxide spin probes.[64] Their molecular structures are reported in Figure 1.

TEMPO molecule is almost spherical in shape, with a van der Waals radius of about 0.34 nm, whereas the cholestane spin probe is quite asymmetric and can be sketched as a prolate ellipsoid with semiaxes of about 0.99 and 0.29 nm, respectively.[65] Their sizes are just across the nanometer length scale that, according to all the recent experiments, characterizes the dynamic heterogeneity and cooperativity in supercooled liquids and polymers on approaching the glass transition. Poly(propylene glycol) of molar mass 4000 g/mol (PPG4000) and T_g = 200 K from Sigma Aldrich was used as received. ESR samples were prepared by mixing two chloroform solutions containing predetermined amounts of polymer and spin probe. The resulting solutions (10^{-3} mol/L) were evaporated to a complete dryness by heating under vacuum for about 120 h.

The values of the principal components of the magnetic tensors are reported in Table 1 and were obtained by a careful

TABLE 1: Values of the Principal Components of Hyperfine and Zeeman Tensors in the Molecular Reference Frame for the Two Different Spin Probes

	A_{xx} (G)	A_{yy} (G)	A_{zz} (G)	g_{xx}	g_{yy}	g_{zz}
TEMPO	33.8	8.0	4.9	2.0019	2.0085	2.0065
cholestane	33.1	5.5	4.5	2.0023	2.0088	2.0065

analysis of the ESR spectrum recorded at 140 K, deeply in the ultraslow regime, according to a procedure detailed elsewhere.[62]

3. Results and Discussion

A suitable description of the rotational dynamics of the TEMPO probe in PPG4000 was achieved by using an isotropic jump model assuming that reorientation takes place by means of almost instantaneous large angle jumps after a mean residence time in a fixed angular site.[66] Key parameters of the model are the mean residence time τ and the mean amplitude of the angular jumps ϕ, from which the rotational correlation times τ_l of the Wigner matrices of rank l can be obtained. As in other glass-forming systems,[58,65] this model was found to improve the agreement between experimental and calculated line shapes with respect to the ordinary diffusion model. A best value of about 70° was found for the mean jump angle ϕ in the whole temperature range. The temperature dependence of the correlation time of rank 2, τ_2, will be used in this work for characterizing the rotational dynamics of TEMPO probe. This choice is due to the well-known sensitivity of the ESR spectroscopy in the higher temperature region to this sole quantity.[55]

On the other hand, for the highly asymmetric cholestane spin probe, a better description of the ESR spectra was obtained by using the anisotropic diffusion model[56,63] with the rotational dynamics described in terms of a spinning ($D_{||}$) and a tumbling ($D_{\perp}$) diffusion constant. Because the anisotropy ratio ($D_{||}/D_{\perp}$) was found to be almost independent of temperature ($D_{||}/D_{\perp} \approx 18$), only the behavior of spinning dynamics will be discussed. To simplify the comparison with the rotational dynamics of TEMPO probe, a spinning correlation time is defined as $\tau_{||} = 1/6D_{||}$. In Figures 2 and 3, some typical ESR line shapes, recorded at different temperatures, are reported for TEMPO and cholestane in PPG4000, respectively. The predictions for the line shapes calculated by using the stochastic models briefly discussed above are also shown as dotted lines. It should be remarked the strong temperature dependence of the ESR line shape and the good capability of the numerical algorithms in reproducing the main spectral details.

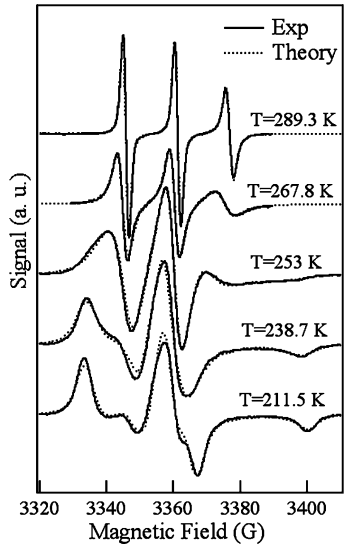

Figure 2. Comparison between ESR experimental and theoretical spectra for TEMPO in PPG4000.

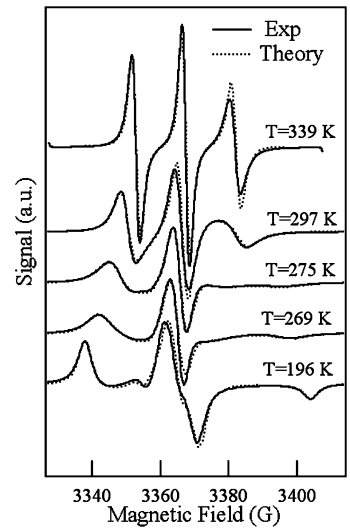

Figure 3. Comparison between ESR experimental and theoretical spectra for cholestane in PPG4000.

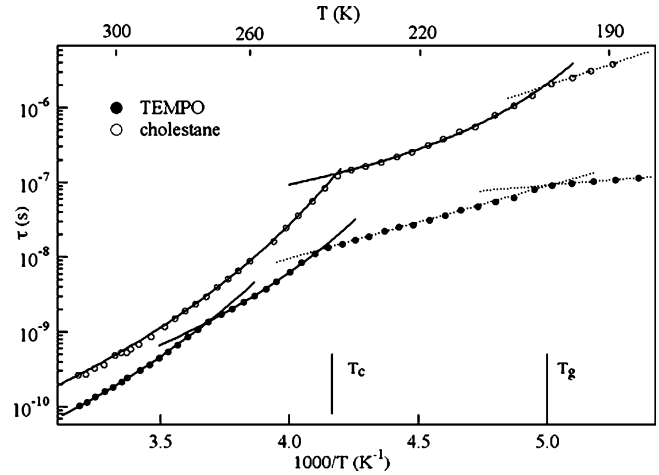

Figure 4. Correlation times τ for TEMPO (●) and cholestane in PPG4000 vs 1000/T. Continuous superimposed lines refer to VF laws, and dotted lines refer to Arrhenius laws.

In Figure 4, the temperature dependences of the rotational correlation times τ of TEMPO and cholestane spin probes in PPG4000 are shown in the overall investigated temperature range. By inspection, cholestane dynamics is slower than TEMPO dynamics; however, the two tracers exhibit similar trends. In particular, dynamical regimes separated by sharp crossovers are observed where the temperature dependence of correlation times (the symbol τ here is used for both τ_2 and $\tau_{||}$) is well reproduced by assuming either Arrhenius behavior:

$$\tau = \tau_{\infty} \cdot \exp\left(\frac{\Delta E}{RT}\right) \quad (1)$$

or Vogel−Fulcher behavior (VF):

$$\tau = \tau_{\infty} \cdot \exp\left(\frac{T_b}{T - T_0}\right) \quad (2)$$

TABLE 2: Fitting Parameters of the Arrhenius and Vogel−Fulcher Equations in the Different Dynamical Regions for Both Spin Probes

probe	temperature range (K)	fit law	ΔE (kJ/mol)	T_b (K)	T_0 (K)	$\log(\tau_\infty$ (s))
TEMPO	$T > 271 \pm 2$	VF		1030 ± 50	162 ± 6	-12.9 ± 0.4
TEMPO	$271 \pm 2 > T > 243 \pm 3$	VF		670 ± 30	163 ± 5	-11.5 ± 0.3
TEMPO	$243 \pm 3 > T > 200 \pm 2$	Arr	19 ± 3			-11.9 ± 0.2
TEMPO	$T < 200 \pm 2$	Arr	5.4 ± 1.0			-8.5 ± 0.1
cholestane	$T > 239 \pm 2$	VF		950 ± 50	163 ± 4	-12.3 ± 0.3
cholestane	$239 \pm 2 > T > 200 \pm 2$	VF		207 ± 15	162 ± 5	-8.05 ± 0.2
cholestane	$T < 200 \pm 2$	Arr	22 ± 4			-11.4 ± 0.3

The values of parameters pertaining to the different regimes are collected in Table 2.

For both molecular probes, a high temperature region exists where the tracer reorientation is closely driven by the dynamics of the polymer backbone. In fact, the temperature dependence of the correlation times is here well described by two VF laws with Vogel temperatures T_0 and pseudoactivation temperatures T_b virtually coincident with the values $T_0 = 163 \pm 2$ K and $T_b = 1174 \pm 80$ K obtained by dielectric spectroscopy measurements on the same polymer.[67]

The difference in the absolute values of the reorientational times of the two tracers in this region could be understood in terms of their different sizes. In the framework of the Rouse model,[49] modes with relaxation time τ extend over regions as wide as $\Delta x \propto (\tau)^{1/4}$. Therefore, by assuming that the two probes are driven by modes of different wavelength, with the scaling $\tau \propto (V)^{4/3}$ and with a rough evaluation of TEMPO and cholestane volumes, the ratio τ(cholestane)/τ(TEMPO) is estimated as ~2.7; this value has to be compared to the experimentally found ratio of about 2.5 in this temperature region.

On lowering temperature and at a characteristic value that is probe-dependent, a first dynamic crossover is found where the tracer rotation decouples from the main relaxation of the polymer backbone. The decoupling, however, is not complete; in fact, the pseudoactivation temperature decreases, but the rotational correlation times continue to follow a VF law with the same Vogel temperature T_0. Consequently, the behavior in these two dynamical regions can be described in terms of the scaling law with respect to the main dielectric α relaxation time τ_α, which results from large-scale conformational rearrangements of the polymer chain backbone:

$$\tau = A \cdot \tau_\alpha^{\xi} \tag{3}$$

The coupling parameter ξ is found to change from about 1 in the highest temperature regions to about 0.6 and 0.2 in the second dynamical region for TEMPO and cholestane respectively. The crossover region is magnified in Figure 5 where the rotational correlation times are directly plotted versus the α relaxation time as obtained from VF parameters of ref 67. By inspection of Figures 4 and 5, it is noted that even if the crossover takes place at a higher temperature for the TEMPO probe, its effect is more effective in the case of the cholestane tracer. Furthermore, for the latter, the power law of eq 3 extends over a wider temperature region approaching the glass transition.

Decouplings of microscopic diffusion from structural relaxation have been observed in many different glass-forming systems with linear and non linear ESR spectroscopy[23,25−28,63,68−70] and with other experimental techniques;[20,21,31,71−74] in several cases, the scaling law of eq 3 was found to hold for both translational and rotational microscopic dynamics. Furthermore, recent theoretical and numerical studies on different glass former models evidenced the presence of decoupling phenomena in transport properties,[40,75−78] invoking a crucial role of the growing length scale typical of the heterogeneous and cooperative character of dynamics. In this respect, the difference in the breaking temperatures exhibited by the two tracers could be quite naturally related to the different length scale on which they probed dynamics.

More in detail, we first consider the case of cholestane tracer in PPG4000; we found the crossover at 240 K (about $1.2 \cdot T_g$) with a value of the rotational correlation time (~10^{-7} s) virtually coincident with the universal "magic" relaxation time $\tau(T_c)$ that, according to Novikov and Sokolov, marks the dynamic crossover from liquid-like to solid-like behavior of glass formers.[18] We found a very similar behavior, with the same probe, in several other polymers such as PMA,[63] PnBA,[28] PEA,[26] and some liquid crystalline polymethacrilates,[79] where the crossover was already ascribed to the onset of cooperativity. In ref 79 by an extension of the Vrentas−Duda[80] phenomenological approach, an estimation of the number of cooperative units was also achieved. It should be emphasized that in all the quoted cases the crossover temperatures were found to be near to the value $1.2 \cdot T_g$ where the critical temperature of MCT is usually found and where, according to many studies,[40−46] dynamical heterogeneities become appreciable on the nanometer length scale.

The universal behavior of the tracer cholestane in the different polymers, together with the differences exhibited by the smallest TEMPO probe in PPG4000, actually support the idea that the observed crossovers are a signature of a growing length scale characterizing some fundamental aspects of dynamics. In this framework, a theoretical physical ground for the interpretation of our experimental results can be found in the recent works of Guenza and co-workers[81−83] attempting to go beyond the Rouse

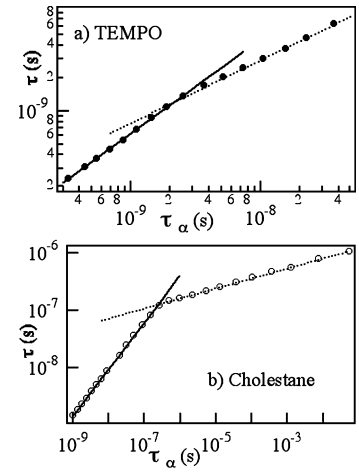

Figure 5. Crossover region for TEMPO (a) and cholestane (b) in PPG4000: correlation times τ vs α relaxation time of PPG4000. Power law fits are superimposed.

model. In these works, a set of coupled generalized Langevin equations were derived starting from the exact Liouville equation and using projector operator techniques, where intramolecular and cooperative intermolecular contributions were explicitly taken into account both in the propagator and in the memory function. In this way, while maintaining the central idea of intrachain relaxation modes, a more complete description of dynamics was proposed thanks to which many of the shortcomings of the Rouse model, numerically and experimentally observed in both local and global chain dynamics, were explained.[83] More importantly, such anomalies were related to the heterogeneous-correlated character of dynamics that, according to the model calculations, arises from the complex interplay between local chain connectivity and intermolecular excluded volume interactions inducing frustration in the fluid.[82] Now it seems feasible to assume that the TEMPO reorientation is more sensitive to local properties of the chain (and eventually to very high index intrachain relaxation modes), whereas the cholestane dynamics is more coupled to the relaxation modes of the chain with low index. In fact, remarkably enough, the TEMPO tracer size is comparable with the length of statistical segment in flows of polymers.[84]

In the very high temperature region, where the polymer shows a homogeneous character with only one relevant time-scale, the dynamics of both tracers follows the same VF law. TEMPO dynamics, however, shows soon some instability, and in a small temperature range the scaling law of eq 3 holds, until at $T \approx$ 240 K a thermally activated regime sets in. Such behavior seems to indicate that the main chain relaxation has become too slow to drive the faster rotational diffusion of the probe. Instead, at this stage, a coupling with less-cooperative and more local relaxation mechanisms could be expected. So much so that it should be emphasized that the value of the activation energy (ΔE of eq 1) was found to be about 19 kJ/mol, comparable with the typical values of the activation energy of β relaxation of polymers.[85] Furthermore, the crossover temperature was virtually coincident with the $\alpha-\beta$ splitting temperature, $T_{\alpha-\beta} \approx$ 239 K, of PPG4000 as estimated by Moon and co-workers with dielectric measurements.

By inspection of Figure 4, one notes that also cholestane spin probe evidences a crossover from VF to Arrhenius behavior, and the activation energy (22 ± 2 kJ/mol) suggests a coupling with β relaxation. However, for cholestane, the crossover was found at a very lower temperature, virtually coincident with the glass transition temperature of the polymer, where the time scale of structural relaxation and tracer reorientation definitively separate. Still this behavior is common to other polymer matrices investigated by ESR with the same probe[26,28,63,70,79] and supports the idea that cholestane reorientation is more efficiently coupled to the relaxation modes of the chains, describable in terms of coarse-grained models. According to the calculations of Guenza,[82] the intermolecular cooperative interactions should affect more dramatically the properties of chain relaxation mode of lower index (larger length scale). This finding appears to be in agreement also with our results; indeed looking at the obtained values of the parameter ξ of eq 3, it is seen that cholestane probe evidenced, in the VF regions, a more prominent change of dynamics with respect to the TEMPO probe.

To conclude this discussion, we observe that TEMPO activated dynamics exhibited a further crossover, located very near to the glass transition, with an appreciable change of activation energy from 19 to about 5 kJ/mol. It should be also emphasized that in a previous ESR investigation with the quite similar TEMPOL probe dissolved in PVAc,[86] some of us

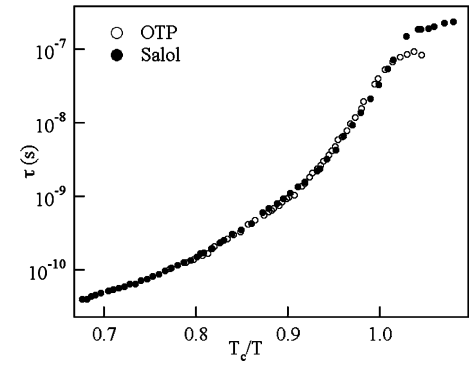

Figure 6. Spinning correlation times of the cholestane probe dissolved in Salol and OTP vs the reduced temperature scale.

detected the $\alpha-\beta$ relaxation splitting followed on cooling by a further Arrhenius regime with a very low value of the activation energy, interpreted as due to the probe coupling with γ relaxation (on the other hand, in such a study the first high temperature crossover was not observed). All these findings support the idea that a sufficiently small tracer probes more local properties of the chains, showing a less universal behavior.

All the results here reported are consistent with the general interpretation of the molecular probe dynamics in polymers where length and time scales play the major role. The TEMPO tracer, due to its subnanometer size, probes dynamics on a fast-time/small-length scale, and it is therefore able to evidence the onset of spatially correlated character of dynamics at temperature higher than cholestane. However, as soon as the β relaxation and the main α relaxation separate following different time scales, TEMPO reorientation tracks in a natural way faster and more local β process. On the contrary, the cholestane spin probe dynamics appears to be more strongly related to the main backbone relaxation. Indeed, the crossover to the β relaxation regime is only observed very near to the glass transition temperature for cholestane; both in PPG4000 and in the other polymers, we previously studied with the same tracer.[26,28,63,70,79] On the other hand, in the crossover VF region, a peculiar dynamical change is observed, where the scaling exponent of eq 3 abruptly decreases. This sharp crossover was evidenced in several different polymers at very similar T/T_g reduced temperature, signaling that the heterogeneous/cooperative character of dynamics of the system has become dominant on the nanometer length scale.

In concluding this work, we briefly recall the results we obtained for the rotational dynamics of the same tracers dissolved in two low molecular inorganic glass formers, namely phenyl-salicylate (Salol) and ortho-therphenyl (OTP).[23,25] For such low molecular systems, where the sole relevant time scale for relaxation is the same as the shear viscosity η, a high temperature region was found for both the tracers where the classical hydrodynamics correctly describes the rotational dynamics through the well-known Debye−Stokes−Einstein (DSE) law, relating the diffusion coefficients to η. In the supercooled region, however, DSE scaling breaks-down, and a power law relates viscosity and diffusion. Finally, at even lower temperatures, activated dynamics sets in. A qualitatively similar scenario was therefore observed with respect to polymers. Another important common feature is found by comparing the behavior of the two tracers in the two inorganic glasses: as in polymers, the cholestane tracer showed a more universal character with respect to TEMPO probe, again signaling that the nanometer length scale plays a major role. In Figure 6, we show the behavior of the rotational correlation times of

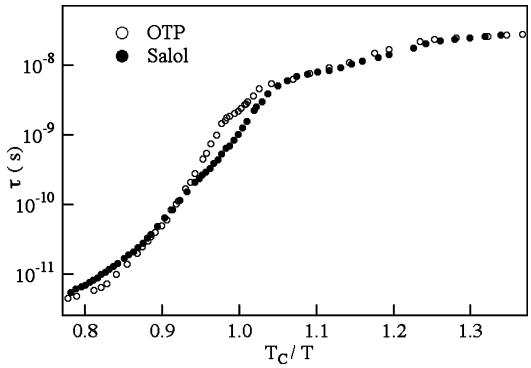

Figure 7. Spinning correlation times of the TEMPO probe dissolved in SALOL and OTP vs the reduced temperature scale.

cholestane tracer in OTP and Salol as a function of the reduced temperature T_c/T, T_c being the mode coupling critical temperature. Because Salol and OTP have comparable fragility indexes, such a scaling provided a collapse of the two shear viscosity temperature dependences.[25] By inspection of Figure 6, it is apparent that the proposed scaling removes almost any differences in the rotational diffusion of cholestane in the two liquids. Quite different results were instead obtained by analyzing the behavior of the TEMPO tracer, as shown in Figure 7. In this case, marked differences can be appreciated just in the crossover region where the decoupling phenomena take place.

Despite these similarities, it should emphasized that the analysis of our experimental data pertaining to polymers is based on the idea that the tracer rotational diffusion is driven by the rheologic relaxation modes of the chain, characterized by different length scales and intrinsically related to the macromolecular nature of these systems. At the same time we point out that, in the case of polymers, we never found the hydrodynamic limit of DSE at variance with low molecular weight glasses. As far as the data pertaining to Salol and OTP are concerned, an attempt to provide a unifying interpretation, accounting also for the different values of the crossover temperatures and power law exponents, has been put forward in terms of the energy landscape paradigm.[87] In this framework, we have just started a systematic study of rotational diffusion of cholestane spin probe dissolved in a series of almost monodisperse PMMA samples of different molecular masses, to highlight the crossover of the diffusion mechanism dependence from on the shear viscosity to on the relaxation modes.

4. Conclusions

The rotational diffusion of two different stiff paramagnetic probes dissolved in PPG4000 has been studied with ESR spectroscopy. Different dynamical regimes, separated by sharp crossovers, have been found, confirming the great ability of the ESR spectroscopy for studying the crossover region of glass-forming systems. The comparison with previous ESR experiments carried out on different polymeric samples highlighted a common scenario when the dynamics of the larger cholestane tracer is considered. The smaller TEMPO probe appears to be more sensitive to the local properties of the chain. However, due to its coupling with the high index chain relaxation modes, it was able to signal the onset of cooperativity at higher temperature than did cholestane. These results strongly support the idea that dynamical decoupling among different transport properties actually derives from development of spatial correlations of mobility on lowering the temperature as suggested by several theoretical and numerical works. The growing of the correspondent dynamic length scale is consequently a universal feature of the physics of glass-forming systems playing a crucial role in the vitrification process.

References and Notes

(1) Brawer, S. *Relaxation in Viscous Liquids and Glasses*; American Ceramic Society: Columbus, OH, 1985.
(2) Debenedetti, P. G. *Metastable Liquids: Concepts and Principles*; Princeton University Press: Princeton, NJ, 1996.
(3) Debenedetti, P. G.; Stillinger, F. H. *Nature (London)* **2001**, *410*, 259–267.
(4) *Proceedings of the 5th International Discussion Meeting on Relaxations in Complex Systems*; Affouard, F., Descamps, M., Ngai, K. L., Eds.; special issues of *J. Non-Cryst. Solids*, 2006; pp 4371−5250.
(5) Dyre, J. C. *Rev. Mod. Phys.* **2006**, *78*, 953–972.
(6) *Proceedings of the 4th Workshop on Nonequilibrium Phenomena in Supercooled Fluids, Glasses and Amorphous Materials, Pisa 17−22 September 2006*; Andreozzi, L., Giordano, M., Leporini, D., Tosi, M., Eds.; special issue of *J. Phys. C: Condens. Matter*, 2007; pp 200301−205149.
(7) Kivelson, S. A.; Tarjus, G. *Nat. Mater.* **2008**, *7*, 831–833.
(8) Adam, G.; Gibbs, J. H. *J. Chem. Phys.* **1965**, *43*, 139–146.
(9) Kivelson, D.; Kivelson, S. A.; Zhao, X. L.; Nussinov, Z.; Tarjus, G. *Physica A* **1995**, *219*, 27–38.
(10) Franz, S.; Parisi, G. *Phys. Rev. Lett.* **1997**, *79*, 2486–2489.
(11) Xia, X.; Wolynes, P. G. *Proc. Natl. Acad. Sci. U.S.A.* **2000**, *97*, 2990–2994.
(12) O'Hern, C. S.; Silbert, L. E.; Liu, A. J.; Nagel, S. R. *Phys. Rev. E* **2003**, *68*, 011306.
(13) Gotze, W.; Sjogren, L. *Rep. Prog. Phys.* **1992**, *55*, 241–376.
(14) Garrahan, J. P.; Chandler, D. *Proc. Natl. Acad. Sci. U.S.A.* **2003**, *100*, 9710–9714.
(15) Biroli, G.; Bouchaud, J. P. *Europhys. Lett.* **2004**, *67*, 21–27.
(16) Whitelam, S.; Berthier, L.; Garraham, J. P. *Phys. Rev. Lett.* **2004**, *92*, 185705.
(17) Beiner, M.; Huth, H.; Schröter, K. *J. Non-Cryst. Solids* **2001**, *279*, 126–135.
(18) Novikov, V. N.; Sokolov, A. P. *Phys. Rev. E* **2003**, *67*, 031507.
(19) Ehlich, D.; Sillescu, H. *Macromolecules* **1990**, *23*, 1600–1610.
(20) Cicerone, M. T.; Blackburn, F. R.; Ediger, M. D. *J. Chem. Phys.* **1995**, *102*, 471–479.
(21) Heuberger, G.; Sillescu, H. *J. Phys. Chem.* **1996**, *100*, 15255–15260.
(22) Hansen, C.; Stickel, F.; Berger, T.; Richert, R.; Fischer, E. W. *J. Chem. Phys.* **1997**, *107*, 1086–1093.
(23) Andreozzi, L.; Di Schino, A.; Giordano, M.; Leporini, D. *Europhys. Lett.* **1997**, *38*, 669–674.
(24) Beiner, M.; Kahle, S.; Hempel, E.; Schröter, K.; Donth, E. *Europhys. Lett.* **1998**, *44*, 321–327.
(25) Andreozzi, L.; Bagnoli, M.; Faetti, M.; Giordano, M. *J. Non-Cryst. Solids* **2002**, *303*, 262–269.
(26) Andreozzi, L.; Faetti, M.; Giordano, M.; Zulli, F. *Philos. Mag.* **2004**, *84*, 1555–1565.
(27) Bartos, J.; Andreozzi, L.; Faetti, M.; Sausa, O.; Racko, D.; Kristiak, J. *J. Non-Cryst. Solids* **2006**, *352*, 4785–4789.
(28) Andreozzi, L.; Autiero, C.; Faetti, M.; Giordano, M.; Zulli, F. *J. Phys.: Condens. Matter* **2006**, *18*, 6481–6492.
(29) Richert, R.; Samwer, K. *New J. Phys.* **2007**, *9*, 36.
(30) Schönhals, A.; Schick, Ch.; Huth, H.; Frick, B.; Mayorova, M.; Zorn, R. *J. Non-Cryst. Solids* **2007**, *353*, 3853–3861.
(31) Corti, H. R.; Frank, A.; Marconi, M. C. *J. Phys. Chem. B* **2008**, *112*, 12899–12906.
(32) Sastry, S.; Debenedetti, P. G.; Stillinger, F. H. *Nature* **1998**, *393*, 554–557.
(33) Sastry, S.; Debenedetti, P. G.; Stillinger, F. H.; Schroder, T. B.; Dyre, J. C.; Glotzer, S. C. *Physica A* **1999**, *270*, 301–308.
(34) Angelani, L.; Di Leonardo, L.; Ruocco, G.; Scala, A.; Sciortino, F. *J. Chem. Phys.* **2002**, *116*, 10297–10306.
(35) Angelani, L.; Ruocco, G.; Sampoli, M.; Sciortino, F. *J. Chem. Phys.* **2003**, *119*, 2120–2126.
(36) Cavagna, A.; Giardina, I.; Parisi, G. *J. Phys. A* **2001**, *34*, 5317–5326.
(37) Schönhals, A.; Kremer, F.; Hofmann, A.; Fischer, E. W.; Schlosser, E. *Phys. Rev. Lett.* **1993**, *70*, 3459–3462.
(38) Ngai, K. L. *Phys. Rev. E* **1998**, *57*, 7346–7349.
(39) Casalini, R.; Ngai, K. L.; Roland, C. M. *Phys. Rev. B* **2003**, *68*, 014201.
(40) Berthier, L. *Phys. Rev. E* **2004**, *69*, 020201(R).
(41) Ediger, M. D. *Annu. Rev. Phys. Chem.* **2000**, *51*, 99–128.
(42) Sillescu, H.; Böhmer, R.; Diezemann, G.; Hinze, G. *J. Non-Cryst. Solids* **2002**, *307*, 16–23.
(43) Schröter, K. *J. Non-Cryst. Solids* **2006**, *352*, 3249–3254.

(44) Donati, C.; Glotzer, S. C.; Poole, P. H.; Kob, W.; Plimpton, S. J. *Phys. Rev. E* **1999**, *60*, 3107–3119.
(45) Doliwa, B.; Heuer, A. *Phys. Rev. E* **2000**, *61*, 6898–6908.
(46) Berthier, L.; Biroli, G.; Bouchaud, J. P.; Cipelletti, L.; El Masri, D.; L'Hôte, D.; Ladieu, F.; Pierno, M. *Science* **2005**, *310*, 1797–1800.
(47) Strobl, G. *The Physics of Polymers*, 2nd ed.; Springer: New York, 1997.
(48) Bird, R. B.; Curtiss, C. F.; Armstrong, R. C.; Hassanger, O. *Dynamics of Polymeric Liquids, Vol. 2 Kinetic Theory*; John Wiley & Sons: New York, 1987.
(49) Doi, M.; Edwards, S. F. *The Theory of Polymer Dynamics*; Oxford University Press: Oxford, 1986.
(50) Pearson, D. S.; Fetters, L. J.; Graessley, W. W.; Strate, G. V.; Von Meerwall, E. *Macromolecules* **1994**, *27*, 711–719.
(51) Paul, W.; Smith, G. D.; Yoon, D. Y.; Farago, B.; Rathgeber, S.; Zirkel, A.; Willner, L.; Richter, D. *Phys. Rev. Lett.* **1998**, *80*, 2346–2349.
(52) Padding, J. T.; Briels, W. J. *J. Chem. Phys.* **2001**, *114*, 8685–8693.
(53) Padding, J. T.; Briels, W. J. *J. Chem. Phys.* **2001**, *115*, 2846–2859.
(54) Guenza, M. *J. Chem. Phys.* **2003**, *119*, 7568–7578.
(55) Muus, L. T.; Atkins, P. W. *Electron Spin Relaxation in Liquids*; Plenum Press: New York, 1972.
(56) Giordano, M.; Grigolini, P.; Leporini, D.; Marin, P. *Adv. Chem. Phys.* **1985**, *62*, 321–388.
(57) Alessi, L.; Andreozzi, L.; Faetti, M.; Leporini, D. *J. Chem. Phys.* **2001**, *114*, 3631–3639.
(58) Andreozzi, L.; Bagnoli, M.; Faetti, M.; Giordano, M. *Philos. Mag. B* **2002**, *82*, 409–419.
(59) Freed, J. H.; Bruno, G. V.; Polnaszek, C. *J. Phys. Chem.* **1971**, *75*, 3385–3399.
(60) Goldman, S. A.; Bruno, G. V.; Polnaszek, C.; Freed, J. H. *J. Chem. Phys.* **1972**, *56*, 716–735.
(61) Hwang, J. S.; Mason, R. P.; Hwang, L. P.; Freed, J. H. *J. Phys. Chem.* **1975**, *79*, 489–511.
(62) Andreozzi, L.; Giordano, M.; Leporini, D. *Appl. Magn. Reson.* **1993**, *4*, 279–295.
(63) Andreozzi, L.; Autiero, C.; Faetti, M.; Giordano, M.; Zulli, F. *J. Non-Cryst. Solids* **2006**, *352*, 5050–5054.
(64) Berliner, L. J. *Spin Labeling Theory and Applications Vol. 1*; Academic Press: New York, 1976.
(65) Andreozzi, L.; Cianflone, F.; Donati, C.; Leporini, D. *J. Phys.: Condens. Matter* **1996**, *8*, 3795–3809.
(66) Ivanov, E. N. *Sov. Phys. JEPT* **1964**, *18*, 1041–1045.
(67) Moon, I. K.; Jeong, Y. H. *Thermochim. Acta* **2001**, *377*, 97–104.
(68) Andreozzi, L.; Faetti, M.; Giordano, M.; Leporini, D. *J. Phys. Chem. B* **1999**, *103*, 4097–4103.
(69) Andreozzi, L.; Faetti, M.; Giordano, M. *J. Non-Cryst. Solids* **2006**, *352*, 3829–3834.
(70) Andreozzi, L.; Autiero, C.; Faetti, M.; Giordano, M.; Zulli, F. *Philos. Mag. B* **2007**, *87*, 799–810.
(71) Rajian, J. R.; Quitevis, E. L. *J. Chem. Phys.* **2007**, *126*, 224506.
(72) Voronel, A.; Veliyulin, E.; Machavariani, V. S.; Kisliuk, A.; Quitmann, D. *Phys. Rev. Lett.* **1998**, *80*, 2630–2633.
(73) Ye, J. Y.; Hattori, T.; Nakatsuka, H. *Phys. Rev. B* **1997**, *56*, 5286–5296.
(74) Hooker, J. C.; Torkelson, J. M. *Macromolecules* **1995**, *28*, 7683–7692.
(75) Bordat, P.; Affouard, F.; Descamps, M.; Müller-Plathe, F. *J. Phys.: Condens. Matter* **2003**, *15*, 5397–5407.
(76) Lombardo, T. G.; Debenedetti, P. G.; Stillinger, F. H. *J. Chem. Phys.* **2006**, *125*, 174507.
(77) Kumar, S. K.; Szamel, G.; Douglas, J. F. *J. Chem. Phys.* **2006**, *124*, 214501.
(78) Chaudhuri, P.; Berthier, L.; Kob, W. *Phys. Rev. lett.* **2007**, *99*, 060604.
(79) Andreozzi, L.; Faetti, M.; Giordano, M.; Palazzuoli, D.; Galli, G. *Macromolecules* **2001**, *34*, 7325–7330.
(80) Vrentas, J. S.; Duda, J. L.; Ling, H. C. *J. Polym. Sci., Polym. Phys. Ed.* **1985**, *23*, 275–288.
(81) Guenza, M. *Macromolecules* **2002**, *35*, 2714–2722.
(82) Guenza, M. *J. Chem. Phys.* **2003**, *119*, 7568–7578.
(83) Zamponi, M.; Wischnewski, A.; Monkenbusch, M.; Willner, L.; Richter, D.; Falus, P.; Farago, B.; Guenza, M. *J. Phys. Chem. B* **2008**, *112*, 16220–16229.
(84) Siline, M.; Arkady, I. L. *Polymer* **2002**, *43*, 5521–5525.
(85) McCrum, N. G.; Read, B. E.; Williams, G. *Anelastic and Dielectric Effects in Polymeric Solids*; Wiley: New York, 1967.
(86) Faetti, M.; Giordano, M.; Leporini, D.; Pardi, L. *Macromolecules* **1999**, *32*, 1876–1882.
(87) Andreozzi, L.; Faetti, M.; Giordano, M. *J. Phys.: Condens. Matter* **2006**, *18*, 931–940.

JP106798C